Axial behaviour of Cantor ring diffractals

2003 J. Opt. A: Pure Appl. Opt. 5 S361

(http://iopscience.iop.org/1464-4258/5/5/392)

INSTITUTE OF PHYSICS PUBLISHING JOURNAL OF OPTICS A: PURE AND APPLIED OPTICS

J. Opt. A: Pure Appl. Opt. **5** (2003) S361–S364 PII: S1464-4258(03)56950-1

Axial behaviour of Cantor ring diffractals

Walter D Furlan[1], **Genaro Saavedra**[1], **Juan A Monsoriu**[2] **and José D Patrignani**[3]

[1] Departamento de Óptica, Universitat de València, E-46100 Burjassot, Spain
[2] Departamento de Física Aplicada, Universidad Politécnica de Valencia, E-46071 Valencia, Spain
[3] Departamento de Física, Universidad Nacional del Sur, 8000 Bahía Blanca, Argentina

Received 22 November 2002, in final form 18 February 2003
Published 22 August 2003
Online at stacks.iop.org/JOptA/5/S361

Abstract
Cantor ring diffractals describe rotationally symmetric pupils constructed from a one-dimensional polyadic Cantor set. The influence on the axial irradiance of several fractal descriptors of such pupils, including fractal dimension, number of gaps and lacunarity, are investigated. It is shown that, contrary to their transversal response, the axial behaviour of these pupils does not resemble the fractal structure of the aperture. The sensitivity of such pupils to the spherical aberration is also analysed.

Keywords: Fractals, Cantor set, lacunarity, impulse response

1. Introduction

In recent years the study of fractals has attracted the attention of several researchers, mainly because many physical phenomena and natural structures can be analysed and described by using a fractal approach [1]. Within this context, the diffraction properties of fractal objects have been studied extensively [2–5]. Due to the complexity of the transmittance of such pupils, the most frequent approach for studying their diffraction patterns is by using numerical calculation. Alternatively, for analysing 1D fractals, an experimental arrangement has been proposed which provides a 2D display, where one axis is associated with the transversal coordinate and the other axis is a certain bounded function of the axial coordinate. This set-up has been shown to be very useful for investigating some general properties of Fresnel diffraction patterns produced by 1D Cantor bars [6].

Recently, a new family of interesting fractal structures—the Cantor ring diffractals (CRDs)—has been introduced [7]. These are 2D rotationally symmetric pupils constructed from polyadic 1D Cantor bars that, in general, are not regular. The characteristics of the diffraction patterns produced by this kind of aperture have been studied in [7]. It was found that, for transversal planes in the far-zone, CRDs display scaling features with spatial frequency that are typical of regular fractal structures. There are, however, other interesting features of the CRDs that have not been investigated and could be significant for future applications. Of particular interest are the focusing properties given by these fractal structures and the influence that optical aberrations have on the axial response. In this work we focused our attention on the intensity distribution that CRDs produce along the optical axis. The axial irradiance given by this kind of pupil with different degrees of lacunarity and their sensitivity to the spherical aberration (SA) are investigated. The study is performed by numerical evaluation of the diffraction integral using an efficient algorithm based on the computation of the CRDs' Wigner distribution function.

2. Cantor ring diffractals

A CRD is a 2D rotationally symmetric pupil that is generated from a 1D Cantor set of a given level of growth. Let us start, for example, from the construction of the polyadic Cantor set shown in figure 1(a). The first step in the construction procedure consists of defining a straight-line segment of unit length called the initiator (stage $S = 0$). Next, at stage $S = 1$ the generator of the set is constructed from N non-overlapping copies of the initiator, each with a scale $r < 1$. At following stages, the generation process is repeated over and over again for each segment in the previous stage. As can be seen in figure 1(a), in addition to N and r a third parameter, ε, is necessary to define the fractal generation uniquely. This parameter, which controls the width of the outermost gap in the first stage, is responsible for the lacunarity of the resulting structure. One of the most frequently used descriptors of fractals, the fractal dimension D, establishes a relation between N and r as $D = \ln(N)/\ln(1/r)$. In figure 1, three-gap Cantor bars are shown for fractal dimension $D = 0.5$ at three stages of growth. According to our previous discussion, it can be seen that, by changing ε, different structures with the same fractal

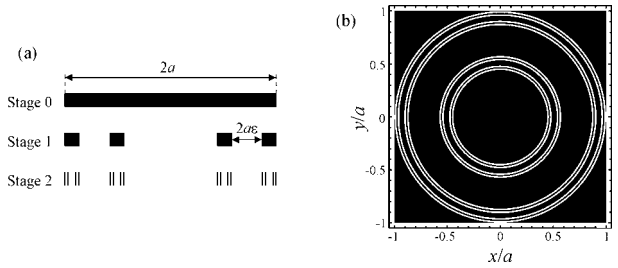

Figure 1. Scheme for the generation of a CRD: (a) construction of the associated Cantor bars from the initator (stage 0), up to stage 2; (b) the pupil transmittance generated from stage 2 in (a). In the figures, the fractal dimension, the lacunarity and the number of segments are $D = 0.5$, $\varepsilon = 0.15$ and $N = 4$, respectively.

dimension can be obtained. Obviously, regular Cantor bars are a sub-class of this generic set that are constructed with all gaps of the same size, consequently showing low lacunarity. A CRD is then a circularly symmetric target that is generated by rotating the Cantor bars (at a given stage) around their mid-point (see figure 1(b)). In summary, the independent variables in the construction of a CRD are the number of stages, the lacunarity, the fractal dimension, and the scale. For this kind of diffractal we will investigate their axial behaviour in the following sections.

3. Intensity along the optical axis

Our plan here is to study the effect of the CRDs as pupils on a generic aberrated system. For the computation of the axial intensity profile we used an efficient numerical technique that was specially adapted for our purposes [8]. In this method the axial intensity given by an optical system is obtained by means of a single integral of a 2D Wigner distribution function associated with the pupil function. As a brief description of this technique, let us consider an optical system with a pupil function $\tau(r, \phi)$, expressed in polar coordinates at the exit pupil plane. According to the Fresnel approximation, the impulse response of the system at different axial points, defined by the values of the defocus coefficient $\delta\omega_{20}$, is given by

$$I(\delta\omega_{20}) = \left| \frac{\delta\omega_{20}}{\lambda} \int_0^{2\pi} \int_0^{\infty} \tau(r, \phi) \times \exp\left\{ \frac{\mathrm{i}2\pi}{\lambda} \omega(r, \phi) + \delta\omega_{20} r^2 \right\} r \, \mathrm{d}r \, \mathrm{d}\phi \right|^2, \quad (1)$$

where $\omega(r, \phi)$ is the wave aberration function and λ is the wavelength of the light. Since we will consider systems suffering only from defocus and primary SA,

$$\omega(r, \phi) = \omega_{40} r^4, \quad (2)$$

where ω_{40} is the SA coefficient. To simplify the numerical computation, the change of variable $t = r^2$ is performed in equation (1). In this way, this equation can be expressed as a function of a single radial integral, as follows:

$$I(\delta\omega_{20}) = \left| \frac{\delta\omega_{20}}{2\lambda} \int_0^{\infty} \tau_0(t) \exp\left(\frac{\mathrm{i}2\pi}{\lambda} \{\delta\omega_{20} t + \omega_{40} t^2\} \right) \mathrm{d}t \right|^2, \quad (3)$$

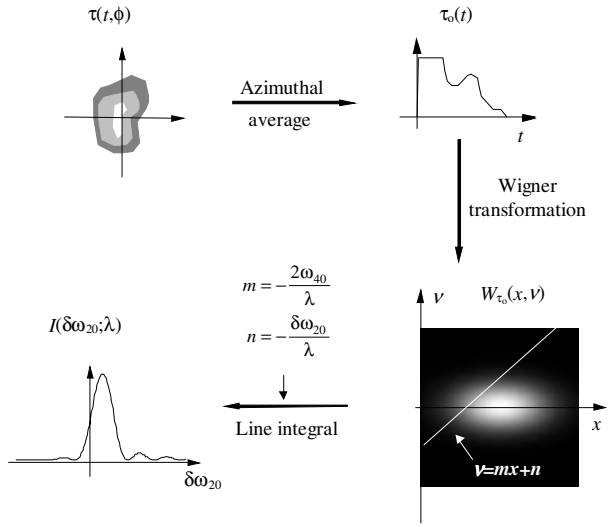

Figure 2. A summary of the procedure for obtaining the axial impulse response of an aberrated system (see [8] for full details).

where $\tau_0(t)$ is the azimuthal average of the pupil function. It was shown in [8] that, after a new change of variables, this result can finally be expressed as

$$I(\delta\omega_{20}) = \left(\frac{\delta\omega_{20}}{2\lambda} \right)^2 \int_{-\infty}^{\infty} W_{\tau_0}\left(x, -\frac{2\omega_{40}}{\lambda} x - \frac{\delta\omega_{20}}{\lambda} \right) \mathrm{d}x, \quad (4)$$

where $W_{\tau_0}(x, \nu)$ is the Wigner distribution function of $\tau_0(t)$

$$W_{\tau_0}(x, \nu) = \int_{-\infty}^{+\infty} \tau_0\left(x + \frac{x'}{2} \right) \tau_0^*\left(x - \frac{x'}{2} \right) \exp(\mathrm{i}2\pi x' \nu) \, \mathrm{d}x'. \quad (5)$$

Figure 2 summarizes schematically the whole procedure for obtaining the axial monochromatic irradiance impulse response using this technique. First, from the 2D pupil function of the system, a 1D azimuthal average $\tau_0(t)$ is obtained. Then the Wigner distribution function of $\tau_0(t)$ is computed. Finally, all the axial irradiances are obtained from this single representation by integrating the values of this function along straight lines in the phase-space domain. The slope and the y-intersects of these lines are given by λ and by the aberration and defocus coefficients—see equation (5)—which are the variable parameters for the computation.

4. Results

The diffracted field along the optical axis was first computed for an unaberrated system by using different members of the family of the CRD in figure 1 as a pupil function. In all cases, the fractal dimension of the Cantor set was $D = 0.5$ and the scale was $r = 1/16$. To explore the typical aspects of fractal structures, we selected the stage of growth S and the lacunarity represented by ε as variable parameters. Figures 3(a) and (b) show the results of the axial irradiance in grey levels for $S = 1$ and 2, respectively. In each picture the irradiances for different values of ε, varying from $\varepsilon_{min} = 0$ to $\varepsilon_{max} = 0.375$, were stacked sequentially to obtain the 2D displays coined *twist plots* [7]. The diffracted field in this case is symmetric around the focus, so only positive

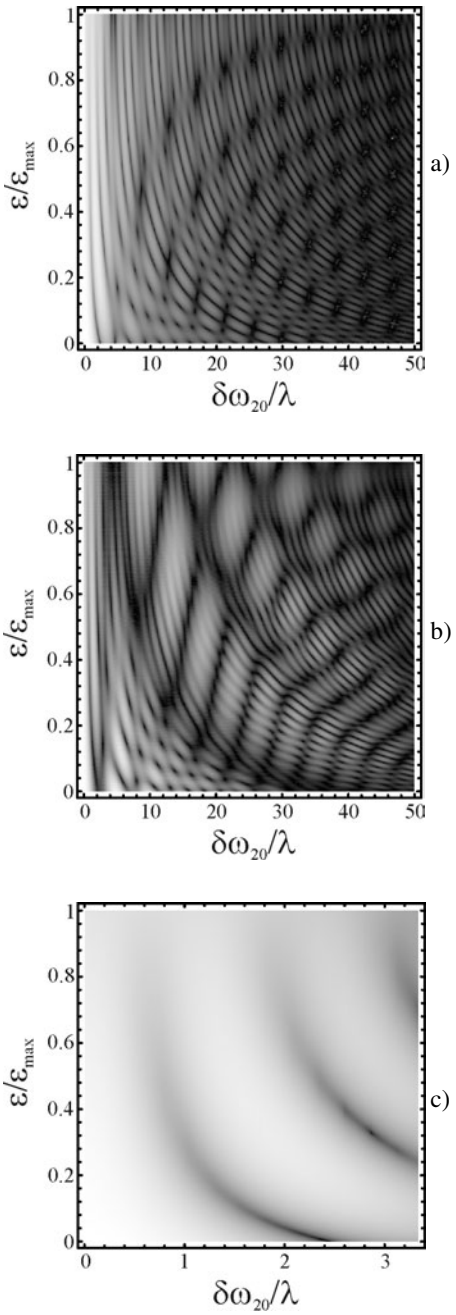

Figure 3. Axial irradiances, in grey levels, given by CRDs constructed with $D = 0.5$ and $N = 4$ and with different lacunarities for $S = 1$ (a) and (c) and $S = 2$ (b). Note that the scale change in the horizontal axis in (c).

values of the defocus coefficient are represented. The most noticeable feature of these plots is the structure of the fringes. These patterns reflect the different locations of the maxima and minima of the axial irradiance obtained for pupils with different lacunarity. Obviously, for each ε the variation in axial intensity is caused by interference from the different rings in the pupil. Despite that previous results indicate that the diffracted far-field intensity in transversal planes can be used to retrieve the dimension of the fractal and other parameters such as the lacunarity, our results show that CRDs do not exhibit fractal behaviour along the optical axis. In fact, for a typical fractal

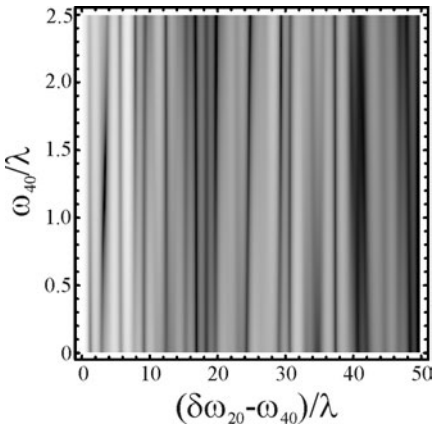

Figure 4. Axial irradiances, in grey levels, given by CRDs constructed with the parameters $D = 0.5$, $N = 4$, $S = 2$ and $\varepsilon/\varepsilon_{max} = 0.1$ as a function of the SA. The axial coordinate is corrected here to avoid the shift that is cited in the main text.

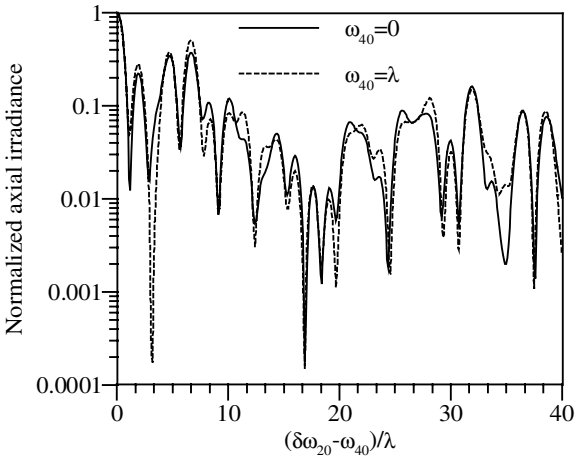

Figure 5. Normalized axial irradiance from figure 4 (horizontal profiles) for $\omega_{40} = 0$ (solid curve) and $\omega_{40} = \lambda$ (dashed curve).

structure the plot for the second stage of growth ($S = 2$) should be similar to a scaled version of the first ($S = 1$) with an overlaid fine structure [7]. However, as can be seen from the comparison of figures 3(b) and (c) (note that the horizontal axis is scaled by r), this is not the case for the axial irradiance. Note, for instance, that the curved patterns originated by the minima in both figures do not coincide.

Our second result arises from the investigation of the sensitivity of this kind of pupil to the SA. To this end, a different kind of representation was used. As shown in figure 4, the axial irradiances for a given CRD ($\varepsilon/\varepsilon_{max} = 0.1$) affected by an SA of varying amount (ranging from $\omega_{40} = 0$ to $\omega_{40} = 2.5\ \lambda$) were now stacked in an orderly way to obtain the 2D display. In the horizontal axis the defocus coefficient was substituted by $(\delta\omega_{20} - \omega_{40})/\lambda$ to avoid the influence of the focal shift caused by the SA [9]. It can be seen that moderate values of SA produce a considerable reduction in the irradiance at certain points of the optical axis—see, for example, the evolution of the axial irradiance for increasing values of the SA around the values $(\delta\omega_{20} - \omega_{40})/\lambda = 4$. This effect can be quantified by inspection of figure 5, where one can notice that, for an SA of $\omega_{40} = \lambda$ (dashed curve) the above-mentioned reduction is of two orders of magnitude. In the same figure, another important

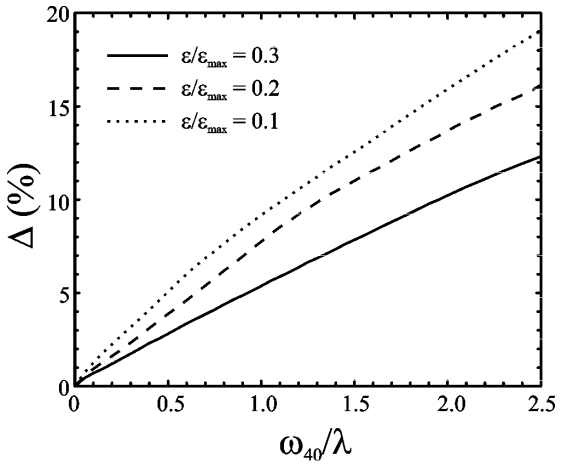

Figure 6. Global relative differences with respect to the unaberrated axial response as a function of the SA, for different values of the lacunarity parameter ε. In all cases, the construction parameters of the CRDs were $D = 0.5$, $N = 4$ and $S = 2$.

reduction can also be observed at $(\delta\omega_{20} - \omega_{40})/\lambda = 20$. A more general approach to quantify the sensitivity of the CRDs to SA can be achieved by defining the following merit function:

$$\Delta(\omega_{40}) = \frac{\int |I(\delta\omega_{20}; \omega_{40}) - I(\delta\omega_{20}; \omega_{40} = 0)| \, \mathrm{d}\delta\omega_{20}}{\int |I(\delta\omega_{20}; \omega_{40} = 0)| \, \mathrm{d}\delta\omega_{20}}, \quad (6)$$

where the integrals are extended to the axial interval of interest. This merit function can be understood as the global relative difference between two axial irradiance profiles as a function of ω_{40}. Then it is a measure of the influence of the SA in the axial response of the CRD being considered. This function was computed for $\varepsilon/\varepsilon_{max} = 0.1$ using the data in figure 5 and for the other two values of ε. The result, shown in figure 6, indicates that, as expected, the sensitivity of the CRDs to the SA depends on the lacunarity. From this figure it is clear that, for a given SA, larger values of ε (lower lacunarity) generate axial irradiance distributions that are more similar to the non-aberrated response. In other words, the sensitivity to SA is a decreasing function of the lacunarity parameter ε.

5. Conclusions

We examined the axial irradiance provided by an aberrated optical system with CRDs as pupil functions. It was found that, contrary to their transversal response, the axial impulse response provided by these pupils does not present a fractal behaviour. Regarding the sensitivity of such pupils to the SA, attention was paid mainly to the influence of the lacunarity in the axial response. As a general result, large values of lacunarity provide an increase in the sensitivity of these pupils to the SA.

Other rotationally symmetric pupil functions with fractal structure are currently being studied. Of particular interest are zone plates with a fractal profile. These fractal zone plates provide an axial response with some interesting features that will be discussed in a forthcoming paper.

Acknowledgment

This research was supported by the Plan Nacional I + D + I (Grant DPI 2000-0774), Ministerio de Ciencia y Tecnología, Spain.

References

[1] Mandelbrot B B 1982 *The Fractal Geometry of Nature* (New York: Freeman)
[2] Allain C and Cloitre M 1986 Optical diffraction on fractals *Phys. Rev.* B **33** 3566–9
[3] Berry M 1979 Diffractals *J. Phys. A: Math. Gen.* **12** 781–97
[4] Sakurada Y, Uozumi J and Asakura T 1992 Fresnel diffraction by 1D regular fractals *Pure Appl. Opt.* **1** 29–40
[5] Alieva T and Agulló-López F 1996 Optical wave propagation of fractal fields *Opt. Commun.* **125** 267–74
[6] Trabocchi O, Granieri S and Furlan W D 2001 Optical propagation of fractal fields. Experimental analysis in a single display *J. Mod. Opt.* **48** 1247–53
[7] Jaggard A D and Jaggard D L 1998 Cantor ring diffractals *Opt. Commun.* **158** 141–8
[8] Furlan W D, Saavedra G, Silvestre E, Andrés P and Yzuel M J 1997 Polychromatic axial behaviour of aberrated optical systems: Wigner distribution function approach *Appl. Opt.* **36** 9146–51
[9] Welford W 1989 *Aberrations of Optical Systems* (Bristol: Institute of Physics Publishing)